Microemulsions of triglyceride and non-ionic surfactant – effect of temperature and aqueous phase composition[α]

Remon F. Joubran*, Donald G. Cornell†, Nicholas Parris

U.S. Department of Agriculture, Agricultural Research Service, Eastern Regional Research Center, 600 East Mermaid Lane, Philadelphia, PA 19118, USA

(Received 15 October 1992; accepted 8 April 1993)

Abstract

The phase behavior of soybean oil, polyoxyethylene (40) sorbitol hexaoleate and water–ethanol was investigated. Regions of water-in-oil (W/O) microemulsions were determined and were found to be strongly dependent on temperature and water : alcohol ratios. At a water : ethanol ratio of 80/20 (wt.%), an oil : surfactant ratio of 2/3 and a temperature of 25°C, the microemulsion region extended continuously from the oil–surfactant axis to the phase diagram center. However, at the hydrophilic–lipophilic balance (HLB) temperature (20–22°C) and a water : ethanol ratio of 80/20 or 75/25 (wt.%), a single-phase area separated from the original microemulsion region. Conductivity measurements and dynamic light scattering intensities at 25°C indicated that association structures were formed with increasing aqueous phase concentrations above 15 wt.%. At 20°C, the single-phase scattering intensities increased sharply with increasing aqueous phase concentrations (38–46 wt.%) and a plateau in the conductivity was detected.

Transmission electron microscopy results supported the finding that more particles are formed with increasing aqueous phase and form connected particles, resulting in constant conductance.

Key words: Aqueous phase composition; Microemulsions; Non-ionic surfactant; Temperature; Triglyceride.

Introduction

Microemulsions are thermodynamically stable, isotropically clear mixtures of water, oil and surfactant, in contrast to "ordinary" emulsions which are turbid and thermodynamically unstable [1]. Microemulsion technology has reached a number of applications, with the main emphasis on the non-polar hydrocarbons [2]; relatively little research has been carried out using more polar oils such as triglycerides [3–10]. One system containing triglyceride, monoglyceride and water has been studied by Larsson and co-workers [3,4] and has ultimately been described as a limited area of water-in-oil (W/O) microemulsion (L_2). Alander and Warenheim [6] have compared triglyceride behavior in microemulsions to ordinary hydrocarbons. They concluded that triglycerides, in particular large triglycerides such as peanut oil, are considerably more difficult to solubilize into microemulsions than hydrocarbons or alkyl esters. Friberg and co-workers [1,5,7] pointed out the difficulties in preparing W/O or oil-in-water (O/W) triglyceride microemulsions by conventional methods. Tricaprylin at a concentration of 13.5 wt.% was solubilized into an O/W microemulsion by using sodium xylene sulfonate as a hydrotrope, and 15 wt.% of solubilized water was achieved by using 50 wt.% surfactant in a water-in-vegetable oil microemulsion. To maximize the microemulsion regions, a different strategy was applied by using a suitable hydrotrope to destabilize the liquid crystalline phase of the triglyceride, surfactant and

*Corresponding author.
†Deceased.
[α]Reference to a brand or firm name does not constitute an endorsement by the U.S. Department of Agriculture over others of a similar nature not mentioned.

water, which leads preferentially to the formation of the microemulsion. Schwab et al. [8] investigated the formation of 1-butanol–triglyceride–aqueous ethanol detergentless microemulsions and associated structures, suggesting microstructures in which oil-rich and water-rich domains were randomly interspersed at equilibrium. Microemulsions of edible oils in a matrix of water and hydrotropes have been reported for food use in the patent literature [11,12].

The present study is concerned with the behavior of microemulsions prepared from triglycerides and other food components. Polyoxyethylene (40) sorbitol hexaoleate (molecular weight, about 3540), a non-ionic surfactant, was selected because of its structural similarity to the continuous phase, and soybean oil was used as a typical triglyceride. Attempts were made to prepare microemulsions containing a minimum amount of oil and surfactant for eventual use as lipid mimetic agents for low-fat foods.

Experimental section

Materials

The surfactant polyoxyethylene (40) sorbitol hexaoleate (Trylox 6746; lot 1J0163) was obtained from Henkel Corporation Emry Group. The soybean oil was obtained from Central Soya Inc., while the cosolvent, ethyl alcohol (200 proof), was purchased from Pharmco Ltd. The potassium chloride (99.5%) was from Merck. All materials were used without further purification. The water was distilled twice and filtered with use of a laboratory reagent grade water system (Continental Water System Corporation, San Antonio, Texas).

Phase Diagrams

Partial phase diagrams were constructed by titrating either soybean oil–surfactant or aqueous phase–surfactant mixtures with water–ethanol solutions or soybean oil, respectively. The phase boundaries of the microemulsion regions were found by visual observation of the change from turbidity to transparency and were checked for anisotropy under polarized light. The microemulsion regions were determined at 20 ± 0.1, 25 ± 0.1 and 30 ± 0.1 °C and at water:ethanol ratios of 60/40, 75/25, 80/20 and 85/15 (wt.%). The three-phase region was determined by weighing samples with water:oil ratios of 1 at various concentrations of surfactant. The samples were incubated at 20 °C until three transparent phases were observed; these were then isolated using a Pasteur pipette. In each phase, the aqueous component was quantitatively evaporated and the oil:surfactant ratios were determined from nuclear magnetic resonance (NMR) calibration curves constructed from signals specific for the oil and surfactant.

Conductivity

The conductivity measurements of the microemulsions were performed by using a conductance meter model 32 YSI Co. equipped with a Pyrex dip cell. The electrodes were platinum–iridium coated with platinum black, and the cell constant was 1 cm. In each experiment, duplicate microemulsion samples were prepared in 50 ml test tubes using 0.5 mM KCl in water–ethanol solution. The samples were placed in a temperature-controlled (± 0.1 °C) water bath for 6 h. The conductance was measured by immersing the electrode into the first test tube for equilibration, and then the conductance value of the second sample was measured and was used to plot conductivity relative to the aqueous phase concentration.

Light scattering

Dynamic light scattering (DLS) measurements were made using a Malvern 4700C spectrometer at different temperatures. The light source was an argon ion laser with an output power of 0.5 W. The scattering intensities and the autocorrelation functions at 60, 75, 90, 105 and 120° were recorded with use of a PCS5 photomultiplier in tandem

with a real-time correlator of 128 channels. The results were scaled to the intensity value of dust-free toluene, which was taken as 1. The cells were cleaned in a NOCHROMIX solution (Godax laboratory), washed with twice-distilled water and were then dried overnight at 80°C. Microemulsion samples were prepared in clean test tubes and were carefully transferred to the clean cells, which were then tightly sealed by plastic caps and placed in the water bath, for 6 h before taking measurements. Care was taken during the sample preparation to use dust-free water.

Freeze-fracture electron microscopy

Samples of microemulsions were thermostatted at 20°C overnight. A portion (2 µl) was placed in a gold specimen holder which was then rapidly plunged into molten Freon-22 on a nitrogen-cooled support. The holder was transferred quickly to the freeze-fracture device (Denton DFE-3) on a vacuum evaporator (Denton DV-502), maintained at −180°C and a pressure of 10^{-6} Torr for 10 min and then fractured by opening. The specimen was etched for 2 min at −98°C at a pressure between 2×10^{-5} and 10^{-6} Torr. The fractured face was immediately shadowed by platinum metal vapor at 45° followed by carbon deposition at 90°. (A resistance monitor, with power cut-off, was used for the automatic regulation of shadow and film thickness). The sample was then melted and washed with twice-distilled water and with hexane. The replica was mounted on 400 mesh copper grid and was examined with use of a Zeiss 10B transmission electron microscope at 60 kV. Photographs were taken at instrumental magnifications of 25000 ×.

Results and discussion

Phase diagrams

The phase behavior of soybean oil, polyoxethylene (40) sorbitol hexaoleate and a water–ethanol mixture (80/20 (wt.%)) at 20°C is demonstrated in Fig. 1. The three-phase region was observed

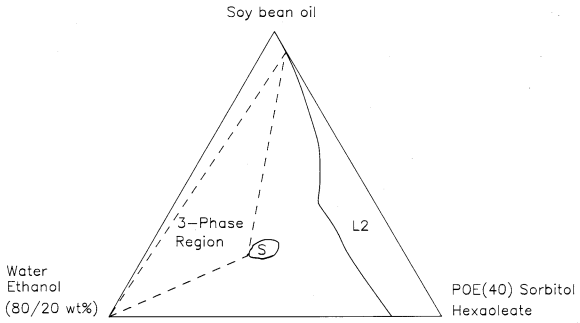

Fig. 1. Isotropic liquid solution regions (L_2 and S) and the three-phase area of the system soybean oil, polyoxyethylene (40) sorbitol hexaoleate and aqueous phase composed of 80/20 (wt.%) water : ethanol at 20°C.

between 20–22°C, i.e. the hydrophilic–lipophilic balance (HLB) temperature or the phase inversion temperature (PIT), at which the hydrophilic and lipophilic properties of the non-ionic surfactant balances. The three-phase region is in equilibrium with the isotropic solution (L_2 phase) and the aqueous phase. The association structure of the single phase (S) is different and cannot be stable on dilution with either oil or water phases [13]. The phase behavior of oil, surfactant and water is very dependent on temperature and the concentration of ethanol. Figure 2 represents the microemulsion regions at different temperatures with a water : alcohol ratio of 80/20 (wt.%). At 30 and

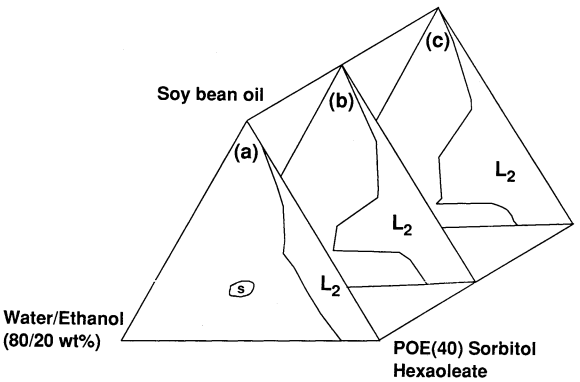

Fig. 2. The effect of various temperatures on the behavior of the isotropic liquid solution regions of the system soybean oil, polyoxyethylene (40) sorbitol hexaoleate and aqueous phase composed of 80/20 (wt.%) water : ethanol at (a) 20°C; (b) 25°C; (c) 30°C.

25°C the system contains a maximum aqueous phase concentration of 39 wt.% and 40 wt.%, respectively with a 2/3 oil:surfactant ratio. Maximum solubilization of the aqueous phase (46 wt.%) at the same oil:surfactant ratio was achieved by reducing the temperature to the PIT. At this temperature, the single-phase region is separated from the original microemulsion and is located in the center of the phase diagram (Fig. 2(a)). At higher temperatures, this isolated area does not exist. The temperature dependence behavior is referable to the ethoxylated surfactant solubility, either in the oil at high temperature or in the water at low temperature. However, at the PIT the solubility is balanced and microemulsion formation is favored. Shinoda and Friberg [14] have pointed out the importance of selecting surfactants with suitable PIT values in order to optimize the conditions and maximize the solubilization of oil and water during the microemulsion preparation.

The effect of changing the water:ethanol composition is summarized in Fig. 3. Changing the concentration of ethanol in the aqueous phase alters the phase behavior. The phase diagram at a water:ethanol ratio of 85/15 (wt.%), with surfactant and oil, shows a classical-shaped W/O microemulsion area (Fig. 3(a)). Increasing the ethanol concentration of the aqueous phase to 20 wt.% resulted in the formation of an isolated area of microemulsion (Fig. 3(b)), which was smaller for 25 wt.% ethanol (Fig. 3(c)). For 40 wt.% ethanol the isolated area was no longer present (Fig. 3(d)) and the surfactant was more soluble in the aqueous phase compared with the solubility at the other three ethanol concentrations.

Light scattering and conductivity

The light scattering and the conductivity results provide valuable information for predicting possible structural behavior upon changing both the temperature and the microemulsion composition. Microemulsion conductivity and light scattering intensities, relative to toluene at 90°, $(Is/It)90$, are plotted against various aqueous phase concentrations at an oil:surfactant ratio of 2/3 at 25°C (Fig. 4). When the aqueous phase concentration was less than 15 wt.% the surfactant was in excess and a few aggregates or inverse micelles were formed [14–15], resulting in an insignificant increase of both the conductivity and the light scattering values. As the aqueous phase concentration was increased from 15 to 35 wt.%, both the conductivity and the light scattering values increased rapidly and typical S-type conduction behavior was observed. The point at which this

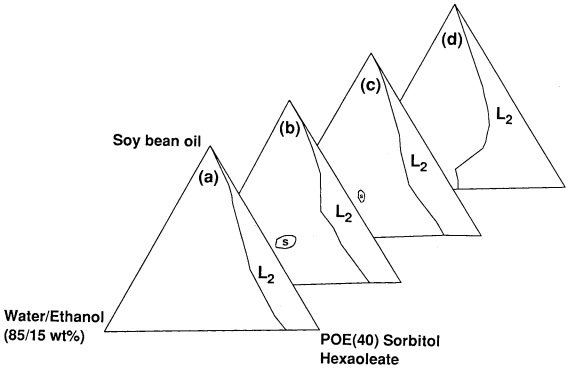

Fig. 3. The effect of changing water:ethanol ratio on the behavior of the isotropic liquid solution regions of the system soybean oil, polyoxyethylene (40) sorbitol hexaoleate and different ratios of water:ethanol: (a) 85/15 (wt.%); (b) 80/20 (wt.%); (c) 75/25 (wt.%); (d) 60/40 (wt.%).

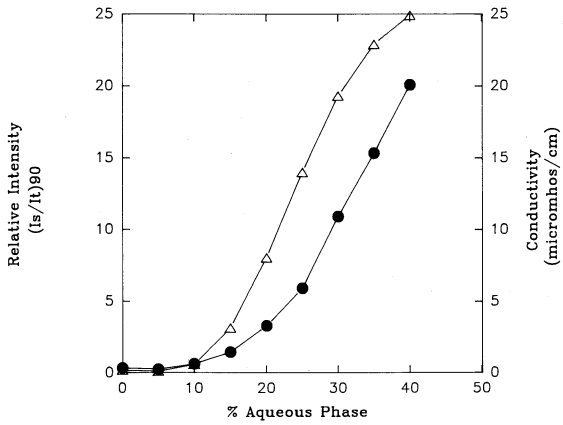

Fig. 4. Conductivity (△) and relative scattering intensities (●) vs. the weight per cent of the microemulsion aqueous phase (the microemulsions were prepared at a constant oil:surfactant ratio of 2/3 at 25°C).

increase begins is denoted as the critical aqueous phase concentration for microemulsion formation [16–19]. The critical surfactant concentration was determined as previously described by Aveyard et al. [20] and was found to be 5 wt.% at 25°C. At 20°C, the microemulsion behavior is significantly different (Fig. 5). At low aqueous phase concentrations, up to 15 wt.%, no difference was observed. In the single-phase region, 38–45 wt.%, a plateau correlation exists between the conductivity and the aqueous phase concentration while the relative scattering intensities increased sharply with increasing aqueous phase. Cazabat et al. [21] have investigated the fluidity of the interfacial region in W/O microemulsions. They concluded that the conductivity of microemulsions increased with attractive interactions between the droplets. During ion transportation through the sample, it is not sufficient to assume that the droplets are in contact, but during collision there is an opening of pores in the interfacial layer and a mixing of their contents. The *Z*-average mean values of the microemulsion particles were obtained from the results of the light scattering measurements. Figure 6 summarizes the values for conductivity and the *Z*-average mean vs. the weight per cent of the aqueous phase prepared at the same oil : surfactant ratio at 25°C. At low aqueous phase concentrations, the conductance is low and the particle size is constant but larger than for particles at high aqueous concentrations. Similar behavior was observed for the conductance and particle size values observed at 20°C (Fig. 7). This transition from aggregates to microemulsion was accompanied by decreasing the *Z*-average mean to about 4.5 nm at an aqueous phase concentration of up to 35 wt.% at both temperatures.

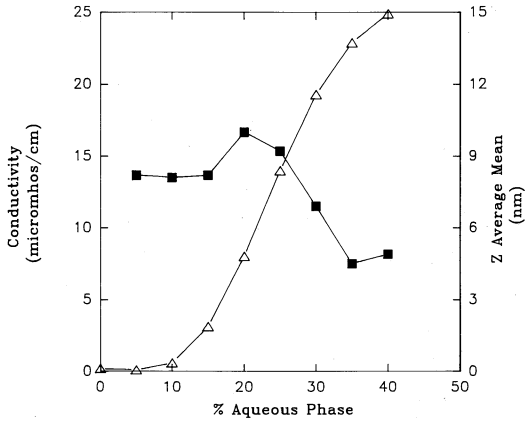

Fig. 6. The *Z*-average mean (■) and conductivity (△) vs. the weight per cent of the microemulsion aqueous phase (the microemulsions were prepared as in Fig. 4, at 25°C).

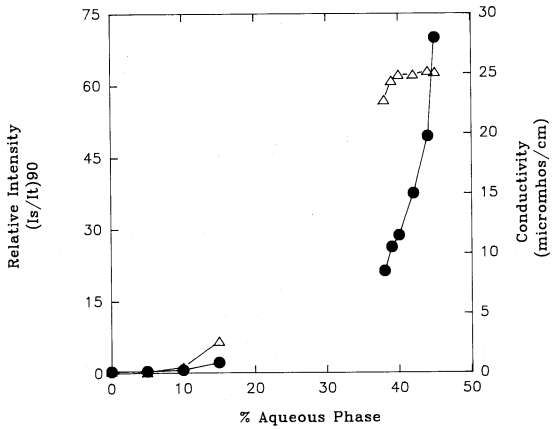

Fig. 5. Conductivity (△) and relative scattering intensities (●) vs. the weight per cent of the microemulsion aqueous phase (the microemulsions were prepared as in Fig. 4, at 20°C).

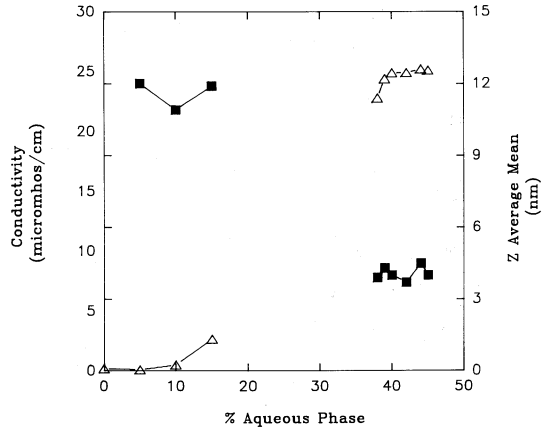

Fig. 7. The *Z*-average mean (■) and conductivity (△) vs. the weight per cent of the microemulsion aqueous phase (the microemulsions were prepared as in Fig. 4, at 20°C).

Transmission electron microscopy (TEM)

Electron microscopy results provided additional information for the existence of certain microemulsion structures [22–25]. TEM can be used as a technique for understanding the behavior of the microemulsion microstructure with changing conditions by comparison of the electron micrographs for three different standards: oil, oil–surfactant, and water–ethanol [23,24]. Figure 8 shows a micrograph of the replica of a W/O microemulsion L_2. Fracture faces of the material were uniform with areas of folded or convoluted sheets (Fig. 8). These areas appear to be randomly stacked (Fig. 8A). The replica of the microemulsion for the isolated area (S) contained a higher concentration of dispersed phase (Fig. 9). The predominant features of the structures in this region are linear and branching chains of disks 40–50 nm in diameter (broad arrows) and areas with a curved outline containing linear chains approximately 5 nm wide (narrow arrows). These interconnected structures appear to form conducting paths of intertwined bicontinuous domains that are similar to the results of Jahn et al. [23].

In conclusion, the results indicate that more particles are formed on increasing the aqueous phase in the system. This causes the formation of connected particles and continuous paths resulting in constant conductance. Further addition of aqueous phase results in phase separation. This interpretation is also supported by electron microscopy studies, which clearly show connected conduit particles and the conducting path (Fig. 9). Evans and co-workers [26,27] have described the percolation-type transition behavior in microemulsions prepared with ionic surfactants, by which they envisage the conducting water paths in bicontinuous systems in terms of chaotic interconnected conduits that are dynamic in nature. Such information concerning microemulsions will provide further knowledge and understanding of the behavior of

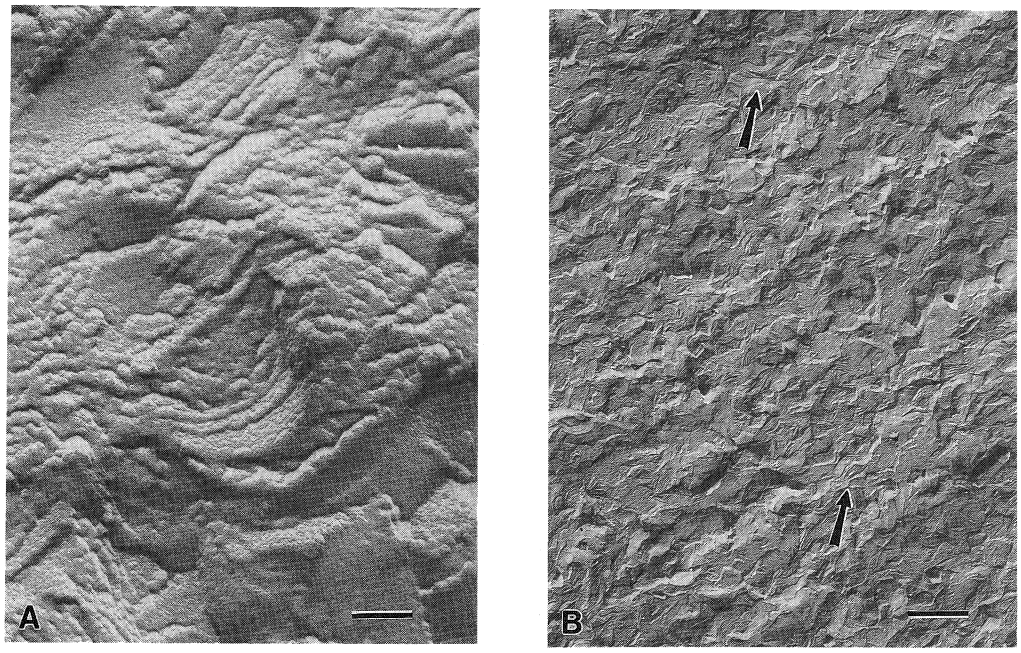

Fig. 8. Replica of the freeze-fractured microemulsion system soybean oil (36 wt.%), polyoxyethylene (40) sorbitol hexaoleate (54 wt.%) and aqueous phase (10 wt.%) comprising 80/20 (wt.%) water:ethanol. (A) Original magnification 100 000 ×; bar represents 100 nm; (B) Original magnification 10 000 ×; bar represents 1 μm, (arrows indicate random stacks of folded or connected sheets).

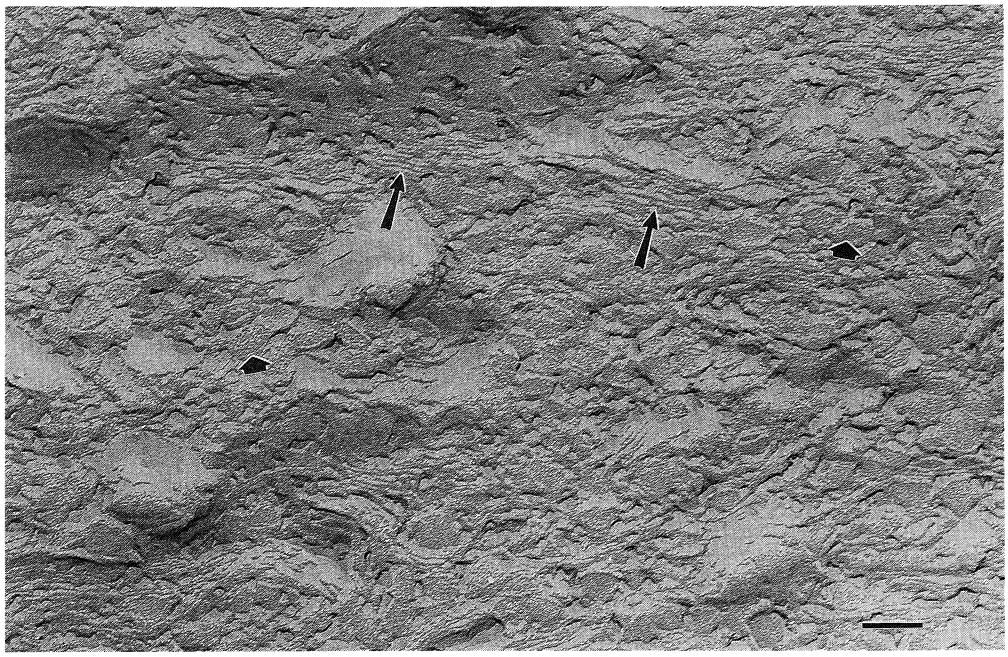

Fig. 9. Replica of the freeze-fractured microemulsion system soybean oil (22.4 wt.%), polyoxyethylene (40) sorbitol hexaoleate (33.6 wt.%) and aqueous phase (44 wt.%) comprising 80/20 (wt.%) water : ethanol: original magnification 100 000 × ; bar represents 100 nm; arrows indicate connected chains or disks.

such triglycerides, in order to enhance their utilization and lipid character in creating prototypes of traditional food systems mimicking high-fat foods.

Acknowledgments

We thank Dr. Peter H. Cooke (ERRC) and Dr. Eric Erbe (SEA, USDA, Beltsville, MD) for their assistance in the electron microscopy studies.

References

1 S.E. Friberg and I. Kayali, in M. El-Nokaly and D. Cornell (Eds.), Microemulsion and Emulsions in Foods, American Chemical Society, Washington, DC, 1991, p. 7.
2 S.E. Friberg and R.L. Venable, in P. Becher (Ed.), Encyclopedia of Emulsion Technology, Vol. 1, Marcel Dekker, New York, 1983, p. 287.
3 T. Gulik-Kyzywicki and K. Larsson, Chem. Phys. Lipids, 35 (1984) 127.
4 M. Lindstrom, H. Ljusberg-Wahren, K. Larsson and B. Borgstrom, Lipids, 16(10) (1981) 749.
5 S.E. Friberg and L. Mandell, J. Am. Oil Chem. Soc., 47(5) (1970) 149.
6 J. Alander and T. Warenheim, J. Am. Oil Chem. Soc., 66(11) (1989) 1656, 1661.
7 S.E. Friberg and L. Rydhag, J. Am. Oil Chem. Soc., 48 (1971) 113.
8 A.W. Schwab, H.C. Nielsen, D.D. Brooks and E.H. Ryde, J. Dispersion Sci. Technol., 4(1) (1983) 1.
9 A.M. Vesala and J.B. Rosenholm, J. Am. Oil Chem. Soc., 62(9) (1985) 1379.
10 L. Hernqvist, in E. Dickinson (Ed.), Food Emulsion and Foam, Royal Society of Chemistry, Leeds, 1986, p. 159.
11 A.W. Peter and J.H. Margaret, U.S. Patent 4 835 002, 1989.
12 E. Magda, D. George and M. Joseph, U.S. Patent 5 045 337, 1991.
13 S. Friberg, I. Lapczynska and G. Gillberg, J. Colloid Interface Sci., 56 (1976) 19.
14 K. Shinoda and S. Friberg, Emulsion and Solubilization, Wiley–Interscience, New York, 1986, Chapter 3.
15 R.C. Baker, A.T. Florence, R.H. Ottewill and Th.F. Tadros, J. Colloid Interface Sci., 100(2) (1984) 332.
16 C. Bond, M. Clausse, B. Lagourette and J. Peyrelasse, J. Phys. Chem., 84 (1980) 1520.
17 M. Lagues and C. Sauterey, J. Phys. Chem., 84 (1980) 3503.
18 E. Sjoblom and S. Friberg, J. Colloid Interface Sci., 62(1) (1978) 16.
19 R. Joubran, R. Patel and S. Friberg, J. Dispersion Sci. Technol., 11(5) (1990) 503.

20 R. Aveyard, P. Binks, S. Clark and P. Fletcher, J. Chem. Tech. Biotechnol., 48 (1990) 161.
21 M. Cazabat, D. Langevin, J. Meunier, O. Abillon and D. Chateray in D. Shah (Ed.), Macro and Microemulsions, American Chemical Society, Washington, DC, 1985, p. 75.
22 J.F. Bodet, J.R. Bellare, H.T. Davis, L.E. Scriven and W.G. Miller, J. Phys. Chem., 92 (1988) 1898.
23 W. Jahn and R. Strey, J. Phys. Chem., 92 (1988) 2294.
24 L.A. Staehelin and W.S. Bertaud, J. Ultrastruct. Res., 37 (1971) 146.
25 S.R. Bellare, H.T. Davis, L.E. Scriven and Y. Talmon, J. Electron Micros. Tech., 10 (1988) 87.
26 S. Chen, D. Evans and B. Ninham, J. Phys. Chem., 88 (1984) 1631.
27 D. Evans, D. Mitchell and B. Ninham, J. Phys. Chem., 90 (1986) 2817.